PHASE ANGLE BASED CORRECTION OF THE MOON MINERALOGY MAPPER RADIANCE MEASUREMENTS. A. Grumpe[1], V. Zirin[1], C. Wöhler[1]; [1]Image Analysis Group, TU Dortmund University, D-44227 Dortmund, Germany; {arne.grumpe | vladimir.zirin | christian.woehler}@tu-dortmund.de.

Introduction: It is well known that the radiance measured by the moon mineralogy mapper (M^3) [1] has been severely distorted by the sensor temperature [2]. A correction based on an area observered under six different sensor temperature conditions has been presented in [2].

Simultaneously, we discovered systematic deviations between normalised reflectance values of the same area derived from images acquired at different phase angles [3]. Due to the high correlation between the phase angle and the sensor temperature, these effects are closely related.

In this work, we present a phase angle based correction approach. Unlike the correction in [2], it relaxes the requirement of all images showing the same surface area. The only requirement is that one pixel-synchroneous image at a reference phase angle is available with other images at arbitrary phase angles. Notably, the phase angle and the sensor temperature may be exchanged because they are highly correlated. We give a phase angle based description due to the development history of our framework.

Normalization: At first, we present the correction model, followed by a description of the fitness function that is minimised. Finally, the optimisation details are explained.

Model: Since the sensor is based on semiconductors, we assume a multiplicative (gain) and an additive (offset) component:

$$E(\alpha) = g(\Delta\alpha)\, E_{\mathrm{obs}} + \mathrm{c}(\Delta\alpha).$$

The real and observed radiances are denoted by E and E_{obs}, respectively. The functions $g(\Delta\alpha)$ and $c(\Delta\alpha)$ represent a temperature/phase angle dependent gain compensation and a temperature/phase angle dependent dark current compensation. Both components are assument to be linear in the phase angle change $\Delta\alpha=\alpha-\alpha_0$, i.e. $g(\Delta\alpha) = g_1\Delta\alpha + g_0$ and $c(\Delta\alpha) = c_1\Delta\alpha + c_0$. The real and the reference phase angle are denoted by α and α_0, respectively. We set $\alpha_0 = 30°$ according to the standard geometry of spectral data [4]. Each wavelength is corrected by a different set of coefficients, respectively.

Fitness function: The fitness function consists of three components

$$F = F_{\mathrm{CR}} + \mu_1 F_{\mathrm{I}} + \mu_2 F_{\mathrm{ref}}$$

with two weighting factors μ_1 and μ_2. The first component F_{CR} measures the deviation of the continuum-removed (CR) reflectance acquired at any phase angle α from the CR reflectance acquired at α_0 and thus emphasises the absorption features:

$$F_{\mathrm{CR}} = \sum_{n_{\mathrm{pix}}} \sum_{n_{\mathrm{chan}}} \left(f_{\mathrm{CR}}\left(f_{\mathrm{norm}}(E(\alpha))\right) - f_{\mathrm{CR}}\left(f_{\mathrm{norm}}(E(\alpha_{\mathrm{ref}}))\right)\right)^2$$

The squared error is computed for all n_{pix} pixels and all n_{chan} senson channels. Consequently, the radiance is photometrically normalised using f_{norm} and then the CR spectrum is computed by f_{CR}. Since the ideal value of α_0 is rarely matched, we allow for a deviation of ±2° and thus refer to the reference phase angle as α_{ref}.

The second component of the fitness function constrains the solution to identity for small deviations of the phase angle, i.e. if the phase angle is close to the reference phase angle, we expect the radiance to be as similar as possible to the observed radiance:

$$F_{\mathrm{I}} = \sum_{n_{\mathrm{pix}}} \sum_{n_{\mathrm{chan}}} \left(f_{\mathrm{norm}}(E(0)) - f_{\mathrm{norm}}(E_{\mathrm{obs}})\right)^2.$$

Since the first components do not cover the absolute reflectance due to the CR spectra, and the second component does not take into account the reference meas-

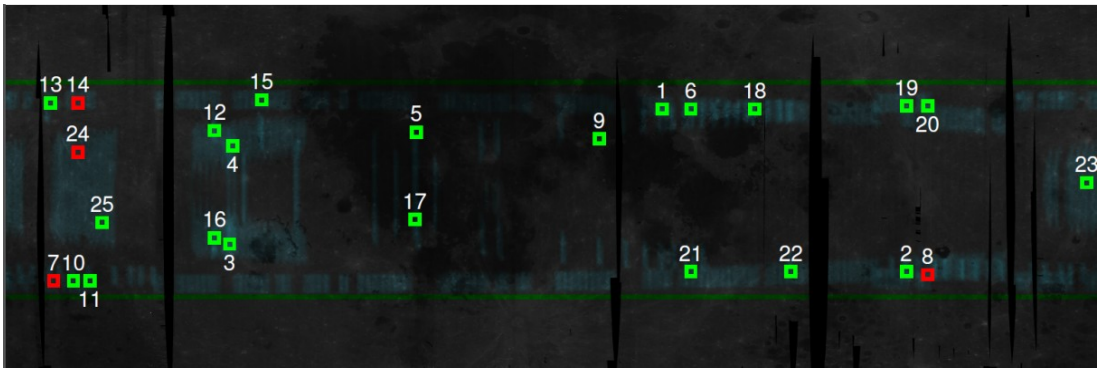

Figure 1: Selected regions. From all regions with images at phase angles 30°±2° we selected 25 regions all over the lunar surface. The regions marked in green are used for the optimisation. The regions marked in red were discarded due to lack of informatien, e.g. single image observations or narrow phase angle ranges.

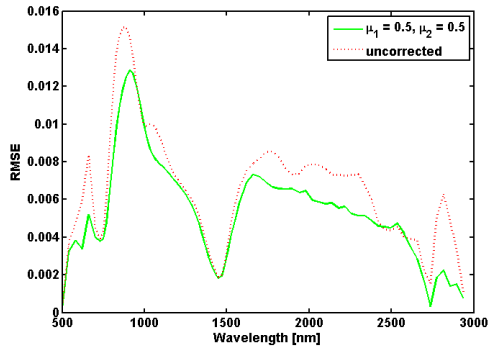

Figure 2: Channelwise RMSE of the uncorrected pixels (red curve) and the result of the correction method (green curve).

urements, we defined the third component

$$F_{\mathrm{I}} = \sum_{n_{\mathrm{pix}}} \sum_{n_{\mathrm{chan}}} \left(f_{\mathrm{norm}}(E(\alpha)) - f_{\mathrm{norm}}(E(\alpha_{\mathrm{ref}})) \right)^2 .$$

Optimization strategy: To normalise the spectral data, we apply the full Hapke model [5], i.e. we divide the radiance by the solar irradiance and fit the single-scattering albedo w of the Hapke model. The remaining parameters are taken from [6]. Thus, the fitness function is highly nonlinear and w depends on the correction. Furthermore, the standard continuum removal approach, i.e. division by the convex hull [7], introduces another nonlinearity.

To linearise the fitness function we propose an interative optimisation. At first, the Hapke model is fit to the current corrected reflectance. Then, the coefficients are updated. This sequential normalisation and coefficient update is repeated until either the fitness function or the coefficients do not change any more.

Additionally, we define a different CR approach. Instead of dividing by the convex hull, we subtract a second order polynomial that fitted to the reflectance data. Similar to the division by the convex hull, this approach eliminates the absolute reflectance and emphasises the absorption bands. Consequently, the fitness function is linear in the channel coefficients and the unique set of new coefficients at each iteration can be determined using linear least squares techniques.

Dataset: From our global M^3 mosaic we selected 25 regions with images at phase angles of 30°±2° as shown in Fig. 1. The regions marked in red were discarded since the phase angle range was too narrow. To avoid the influence of the surface topography, we selected pixels with surface slopes less than 2°.

Results: The channelwise root-mean-squared difference (RMSE) between the CR-spectra of each pixel and its corresponding reference CR spectrum is shown in Fig. 2. Notably, we computed the RMSE using continuum removal based on the convex hull. Thus, the parabolic fit linearisation reduces the RMSE successfully. According to Fig. 3, the band depth of the ferrous absorption trough near 1000 nm significantly depends on the correction. Consequently, a geological interpretation of the spectra should be avoided without proper correction for sensor temperature/phase angle.

Conclusion: We have presented a method to compensate the spectral distortion with respect to the CR spectrum. The presented method efficiently linearises the highly nonlinear optimisation problem and produces plausible results. It does not require all data to overlap at the same region and relies on the existence of data acquired at a reference phase angle/detectore temperature. Finally, we have shown the strong influence of the distortion due to sensor temperature/phase angle on the derived absorption band depth.

References: [1] Pieters et al. (2009) *Current Science* 96(4), 500–505; [2] Lundeen, S. et al. (2011) *PDS Document*, Jet Propulsion Laboratory, JPL D-39032, Version 9.10; [3] Grumpe, A. et al. (2013) *LPS XXXXIV*, abstract # 2267; [4] Pieters, C. M. (1999) *Proc. Workshop on New Views of the Moon II*, abstract #8025; [5] Hapke, B. (2002) *Icarus* 157(2), 523-534; [6] Warell, J. (2004) *Icarus* 167, 271-286; [7] Fu, Z. et al. (2007) *IEEE Trans. Geoscience and Remote Sensing* 45(11), 3827-3844.

Acknowledgement: We would like to thank the LiDO HPC cluster team at TU Dortmund for their support.

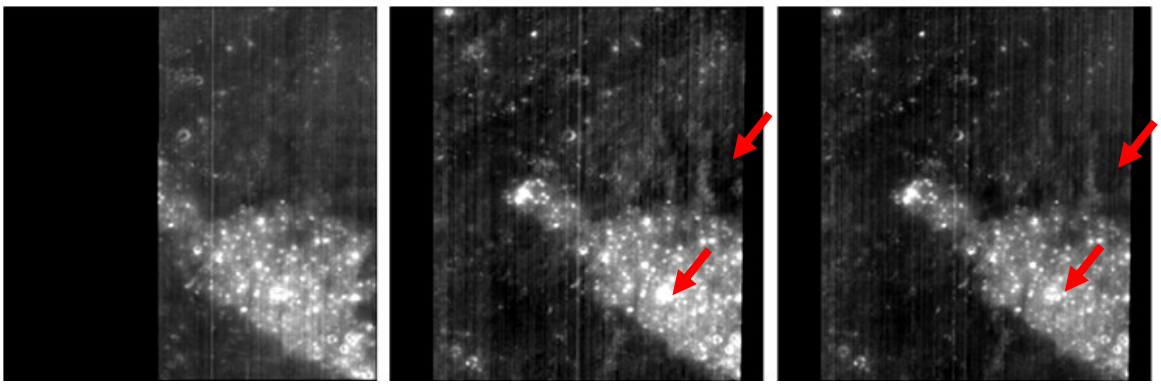

Figure 3: Influence of the correction on the band depth of the ferrous absorption trough near 1000 nm. Left: Reference image at 30.8° phase angle. Centre: Uncorrected image at 52.2° phase angle. Right: Corrected image. The northeastern marked region is more homogeneous after the correction, and the intensity and structure of the bright area marked by the lower arrow closely match the reference.